

Lyman- α coupling and heating during Cosmic Dawn

Shikhar Mittal^{1*} and Girish Kulkarni^{1†}

¹ *Tata Institute of Fundamental Research, Homi Bhabha Road, Mumbai 400005, India*

Accepted —. Received —; in original form —

ABSTRACT

The global 21 cm signal from the cosmic dawn is affected by a variety of heating and cooling processes. We investigate the impact of heating due to Lyman- α ($\text{Ly}\alpha$) photons on the global 21 cm signal during cosmic dawn using an analytical expression of the spectrum around the Lyman- α resonance based on the so-called ‘wing approximation’. We derive a new expression for the scattering correction and for the first time give a simple close-form expression for the cooling due to injected $\text{Ly}\alpha$ photons. We perform a short parameter study by varying the $\text{Ly}\alpha$ background intensity by four orders of magnitude and establish that a strong $\text{Ly}\alpha$ background is necessary, though not sufficient, in order to reproduce the recently detected stronger-than-expected 21 cm signal by the EDGES Collaboration. We show that the magnitude of this $\text{Ly}\alpha$ heating is smaller than previously estimated in the literature by an order of magnitude or more. As a result, even a strong $\text{Ly}\alpha$ background is consistent with the EDGES measurement of the global 21 cm absorption signal.

Key words: radiative transfer – galaxies: formation – intergalactic medium – dark ages, reionization, first stars – cosmology: theory.

1 INTRODUCTION

The 21 cm signal, which arises due to the hyperfine splitting of the ground state of neutral hydrogen atom, is a promising probe of the cosmic dawn and the epoch of reionisation (EoR) (Madau et al. 1997). The interaction of the magnetic dipole moment of the proton and that of the electron splits the ground state of the hydrogen atom into two levels separated by a small energy of $\Delta E = hc/\lambda_{21}$, where $\lambda_{21} = 0.21$ m (Woodgate 1983). Cosmology using the 21 cm line is reviewed extensively by Barkana & Loeb (2001), Furlanetto et al. (2006), and Pritchard & Loeb (2012).

The strength of the 21 cm signal depends on various astrophysical and cosmological processes, many of which are poorly understood. It captures the thermal and ionisation status of the Universe which in turn are a probe of the formation of first stars (Barkana 2018a; Mesinger 2019). An important process in the affecting the 21 cm signal is the Wouthuysen-Field (WF) effect (Field 1958; Wouthuysen 1952). It is created by the Lyman- α from the first luminous sources. This effect makes the 21-cm signal distinguishable from the cosmic microwave background (CMB).

Investigation into the physics of the global 21 cm cosmological signal has recently been re-energised due to detection of a 21 cm signal at redshift $z \sim 17$ by the Experiment to Detect the Global EoR Signal (EDGES) collaboration (Bowman et al. 2018). The detection reported has an amplitude that is more than double of that predicted by the most optimistic

theoretical models. While the cosmological nature of this signal is still being investigated (Hills et al. 2018; Bradley et al. 2019; Singh & Subrahmanyam 2019; Sims & Pober 2019), there have been many new exciting theories which try to explain its anomalous amplitude. Broadly speaking there are two types of ideas in the literature. The first type considers lower matter temperature than the estimates of adiabatic cooling (Barkana 2018b; Berlin et al. 2018; Muñoz & Loeb 2018; Liu et al. 2019). A recent paper by Datta et al. (2020) also explores implications of such excess cooling for the otherwise well-established recombination physics (Seager et al. 1999, 2000). The second type considers an excess radio background above the CMB (Feng & Holder 2018; Ewall-Wice et al. 2018; Fialkov & Barkana 2019; Ewall-Wice et al. 2019). The end result of both the theories is an increase in the amplitude of the predicted 21-cm absorption signal.

Several groups are working to validate the EDGES claim. Some projects that are already active or under development are the Large Aperture Experiment to Detect the Dark Ages (LEDA, Bernardi et al. 2015, 2016; Price et al. 2018), the Shaped Antenna measurement of the background Radio Spectrum (SARAS, Patra et al. 2013; Singh et al. 2017), Probing Radio Intensity at high-Z from Marion (PRIZM, Philip et al. 2019), Radio Experiment for the Analysis of Cosmic Hydrogen¹ (REACH, de Lera Acedo 2019), Sonda Cosmológica de las Islas para la Detección de Hidrógeno Neutro (SCI-HI, Voytek et al. 2014), Zero-spacing Interferometer Measurements of the Background Radio Spectrum (ZEBRA,

* E-mail: shikhar.mittal@tifr.res.in

† E-mail: kulkarni@theory.tifr.res.in

¹ <https://www.kicc.cam.ac.uk/projects/reach>

(Mahesh et al. 2014) and the Cosmic Twilight Polarimeter (CTP, Nhan et al. 2017, 2019).

In this paper we reconsider the effect of Ly α photons on the global 21 cm cosmological signal. We compute the amount of scattering and heating expected from Ly α photons at cosmic dawn. In the process, we derive a new expression for the scattering correction and give a simple closed form expression for the cooling part due to the injected Ly α photons. In order to understand constraints on the high-redshift Ly α background due to the EDGES measurement, we perform a simple single-parameter study where we vary the strength of Ly α radiation background by 4 orders of magnitude to see its effect on the temperature of intergalactic medium (IGM) and correspondingly the differential brightness temperature. Because our purpose here is to gauge the effects of Ly α radiation only, we do not include processes such as X-ray heating (for e.g. Mesinger et al. 2011), shock heating (Furlanetto & Loeb 2004), etc. The redshift range of our interest is $14 \leq z \leq 30$.

Ly α scattering and heating have been considered in the literature before. Field (1958) presented the earliest treatment, in which there was no Ly α heating since it was assumed there are no spectral distortions in the Ly α spectrum. Madau et al. (1997) improved this by accounting for the latter but considered the hydrogen atoms to be at rest, which overestimated the Ly α heating. The first major improvement in the problem came from Chen & Miralda-Escude (2004, hereafter CM04) who solved an appropriate radiative transfer equation numerically. Furlanetto & Pritchard (2006, hereafter FP06) gave analytical estimates using the analytical solutions of Chuzhoy & Shapiro (2006) based on a further approximation called the wing approximation. Recently Ghara & Mellema (2019, hereafter GM19) applied the methods of Chuzhoy & Shapiro (2007) to study the 21 cm signal during the cosmic dawn. According to them, a strong Ly α background radiation is ruled out in view of the EDGES claim.

This paper is organized as follows. In Section 2 we present the theory of scattering and heating by Ly α photons and their effect on the 21 cm signal. In Section 3 we present our results and analysis. We discuss our conclusions and ideas on further work in Section 4. The following cosmological parameters are used: $\Omega_m = 0.32$, $\Omega_b = 0.049$, $\Omega_\Lambda = 0.68$, $h = 0.67$, $Y_p = 0.24$, $T_0 = 2.73$ K, $\sigma_8 = 0.83$ and $n_s = 0.96$ (Planck Collaboration et al. 2016), where T_0 and Y_p are the cosmic microwave background (CMB) temperature measured today and helium fraction by mass, respectively. Unless stated otherwise, we will work in SI units. The reader is cautioned here as they may find some of our expressions differing from those in previous literature, which use CGS units, by a factor of $4\pi\epsilon_0$.

2 THEORY AND METHODS

We begin by writing down the observable 21 cm signal or the differential brightness temperature, which is the spin temperature (T_s) measured against the CMB temperature (T_γ) and is given by (Furlanetto 2006)

$$\Delta T_b = 27\bar{x}_{\text{HI}} \left(\frac{1 - Y_p}{0.76} \right) \left(\frac{\Omega_b h^2}{0.023} \right) \sqrt{\frac{0.15}{\Omega_m h^2} \frac{1+z}{10}} \times \left(1 - \frac{T_\gamma}{T_s} \right) \text{mK}, \quad (1)$$

where z is the redshift, $x_{\text{HI}} \equiv n_{\text{HI}}/n_{\text{H}}$ is the ratio of number densities of neutral hydrogen (HI) and total hydrogen (H), and we have assumed a matter dominated Universe, so that $H(z) = H_0 \sqrt{\Omega_m(1+z)^3}$. The signal is seen in absorption when $\Delta T_b < 0$ and when $\Delta T_b > 0$ the signal is seen in emission. [Note that in Equation (1) we write h to represent the Hubble's constant in units of $100 \text{ km s}^{-1} \text{ Mpc}^{-1}$ for the last time. From here onwards h will denote Planck's constant.]

Before reionization, the globally averaged neutral hydrogen fraction is same as that measured in the bulk of intergalactic medium (IGM), so that $\bar{x}_{\text{HI}} = x_{\text{HI}}$. Moreover, neglecting the electron contribution from helium, it is safe to write

$$x_{\text{HI}} = 1 - x_e, \quad (2)$$

where $x_e \equiv n_e/n_{\text{H}}$ is ratio of number of electrons to the total number of hydrogen atoms. We obtain the x_e values for our cosmology at high redshifts using the RECFAST code² (Seager et al. 1999).

The spin temperature is defined as the temperature required to achieve a given ratio of populations of upper and lower hyperfine levels, i.e.,

$$\frac{n_1}{n_0} \equiv 3e^{-T_*/T_s}, \quad (3)$$

where $T_* = h\nu_{21}/k_B = 0.068$ K, h is the Planck's constant, k_B is the Boltzmann constant and $\nu_{21} = 1420$ MHz. The factor of 3 is due to the degeneracy factor. The interaction of HI with the CMB photons, collisions with the other hydrogen atoms/electrons, and the interaction of Ly α photons determines T_s (Field 1958). As a result, it can be expressed as a weighted arithmetic mean of T_γ , T_K and T_α which represent the CMB temperature, gas kinetic temperature and colour temperature, respectively (Furlanetto 2006). Thus,

$$T_s^{-1} = \frac{T_\gamma^{-1} + x_K T_K^{-1} + x_\alpha T_\alpha^{-1}}{1 + x_K + x_\alpha}. \quad (4)$$

where the collisional coupling and Ly α coupling are

$$x_K = \frac{T_* C_{10}}{T_\gamma A_{21}}, \quad (5)$$

$$x_\alpha = \frac{T_* P_{10}}{T_\gamma A_{21}}, \quad (6)$$

respectively. Here, C_{10} and P_{10} are the de-excitation rates by collisions and Ly α photons, respectively, and $A_{21} = 2.85 \times 10^{-15}$ Hz is the Einstein coefficient of spontaneous emission for the hyperfine transition. The de-excitation rate C_{10} can be written as $n_e \kappa_{e\text{H}} + n_{\text{H}} \kappa_{\text{HH}}$, where n_i is the number density of species i and κ_{ij} is the specific rate coefficient in units of volume per unit time. The empirically derived expression for them as a function of temperature can be found in Liszt (2001). So the final expression for x_K is

$$x_K(z) = \frac{T_* n_{\text{H}}}{T_\gamma A_{21}} (x_e \kappa_{e\text{H}} + \kappa_{\text{HH}}). \quad (7)$$

For more details of x_K see Pritchard & Furlanetto (2007).

The variation of gas kinetic temperature with redshift is important in the understanding of the 21 cm signal. For this we use the following thermal equation

$$(1+z) \frac{dT_K}{dz} = 2T_K - \frac{T_K(1+z)}{1+x_{\text{He}}+x_e} \frac{dx_e}{dz} - \frac{2}{3nk_B H} \sum q, \quad (8)$$

² <https://www.astro.ubc.ca/people/scott/recfast.html>.

where $n = n_{\text{H}}(1 + x_{\text{He}} + x_{\text{e}})$ is the total particle number density and similar to x_{e} , we can define x_{He} . For the given cosmological parameter Y_{p} it is

$$x_{\text{He}} = \frac{Y_{\text{p}}}{4(1 - Y_{\text{p}})}. \quad (9)$$

Note that both q and n_{H} should either be in comoving units or both in proper units. The Equation (8) is the most general form of thermal evolution, however, for the redshifts of our interest the second term on the right hand side may be dropped since the electron fraction changes negligibly. Also, because the x_{e} itself is quite small ($\sim 10^{-4}$), the Compton heating may be neglected (Seager et al. 1999, 2000; Ali-Haïmoud et al. 2014). Thus, in this work we will consider only the Ly α heating term. We will integrate the Equation (8) from $z = 30$ to $z = 14$ with the initial condition, obtained from RECFAST, $T_{\text{K}}(z = 30) = 18 \text{ K}$.

2.1 Effect of Scattering of Ly α Photons

The ultraviolet (UV) photons are released into the IGM by the radiations from the stars and galaxies in the late Universe ($z \lesssim 50$). Of particular interest here are the Ly α photons. They play a dual role in the physics of the 21 cm signal. First, the Ly α background couples the 21 cm spin temperature to the gas kinetic temperature. Second, it also changes the gas temperature, usually heating the gas. We discuss the coupling in this section.

An excitation followed by a de-excitation due to scattering of UV photons can cause hyperfine transitions in H I. For e.g., a hydrogen atom in the first excited state may return to a different hyperfine state it originally started from. The photons so involved are from the Lyman series. This effect is called the Wouthuysen-Field effect (as mentioned in the introduction). Naturally, there is some energy exchange in this process between the two species and as a result the system tends to achieve an equilibrium. The ‘heat reservoir’ of the Ly α photons can be given an artificial temperature called the colour temperature (Madau et al. 1997).

The over-simplified picture presented above would imply $T_{\alpha} = T_{\text{K}}$ (Field 1958) but this is assuming that there are no spectral distortions in Ly α spectrum. Over the years the model for x_{α} and T_{α} have been improved. Some of the obvious corrections would be the following. Firstly, due to scattering the specific intensity goes down in the vicinity of Ly α resonance and so does x_{α} . Moreover, the energy exchange between H I and Ly α photons causes T_{α} not to relax to T_{K} but to somewhere between T_{K} and T_{s} (CM04). Further details such as fine and hyperfine structure of Ly α and frequency dependence of spin flip probability have been considered in Hirata (2006, hereafter H06).

To evaluate x_{α} and T_{α} we need the specific intensity of Ly α photons denoted by $J(\nu)$ (sometimes denoted as J_{ν}). Here we define it in terms of number (*not* energy) per unit proper area per unit proper time per unit frequency per unit solid angle. It is obtained by solving the equation of radiative transfer under the Fokker-Planck approximation (Rybicki & dell’Antonio 1994). Even then it is generally not possible to find analytical expressions for x_{α} and T_{α} . The results of CM04 and H06 are quite accurate but they rely on numerical approach and iterative techniques. A different approach

was taken by Meiksin (2006) who solved the radiative transfer equation for a two-level atom without the Fokker-Planck approximation. For our work we use the analytical solution for the spectrum around a general resonance line under the ‘wing approximation’ by Grachev (1989) or more specifically the work of Chuzhoy & Shapiro (2006) for Ly α photons. In the wing approximation the Voigt line profile is approximated by the ‘wings’ of the Lorentzian line (see FP06).

We now present the spectrum of Ly α radiation. For mathematical convenience the linearity of equation of radiative transfer, under the Fokker-Planck approximation, allows us to split the solution into two parts: spectrum of continuum photons $J_{\text{c}}(\nu)$ and that of injected photons $J_{\text{i}}(\nu)$, so that $J = J_{\text{c}} + J_{\text{i}}$. Physically, the difference between the two lies in their origin. The photons released by the stars between the Ly α and Ly β which redshift and ultimately give Ly α photons are called continuum photons. The photons between Ly γ and Ly ∞ will redshift to Ly γ or other higher Lyman series lines. These higher Lyman lines can decay to Ly α photons via radiative cascade. These comprise the injected photons. Let the undisturbed background Ly α specific intensity far from the resonance line be $J_{\alpha} = J_{\alpha}(z)$ (we will discuss its calculation in Section 2.3) and for now we assume that it is same for both, the continuum and injected photons. The specific intensity of continuum photons is³

$$J_{\text{c}}(x) = \frac{2\pi J_{\alpha}}{a\tau_{\alpha}} \exp \left[-2\eta x - \frac{2\pi x^3}{3a\tau_{\alpha}} \right] \times \int_{-\infty}^x y^2 \exp \left[2\eta y + \frac{2\pi y^3}{3a\tau_{\alpha}} \right] dy, \quad (10)$$

and for injected photons

$$J_{\text{i}}(x) = J_{\text{i}}(0) \exp \left[-2\eta x - \frac{2\pi x^3}{3a\tau_{\alpha}} \right] \text{ for } x \geq 0 \quad (11)$$

whereas for $x < 0$ it is the same as $J_{\text{c}}(x)$. The changed variable, Voigt parameter⁴, Doppler width and the recoil parameter are given by

$$x = \frac{\nu - \nu_{\alpha}}{\Delta\nu_{\text{D}}}, \quad (12)$$

$$a = \frac{A_{\alpha}}{4\pi\Delta\nu_{\text{D}}}, \quad (13)$$

$$\Delta\nu_{\text{D}} = \nu_{\alpha} \sqrt{\frac{2k_{\text{B}}T_{\text{K}}}{m_{\text{H}}c^2}}, \quad (14)$$

$$\eta = \frac{h/\lambda_{\alpha}}{\sqrt{2m_{\text{H}}k_{\text{B}}T_{\text{K}}}}, \quad (15)$$

respectively. Here $A_{\alpha} = 6.25 \times 10^8 \text{ Hz}$ is the Einstein spontaneous emission coefficient of Ly α transition, m_{H} is the mass of recoiling atom (here hydrogen), $\lambda_{\alpha}(\nu_{\alpha})$ is the wavelength (frequency) of the Ly α photon, c is the speed of light and the Ly α optical depth (Gunn & Peterson 1965) is given by

$$\tau_{\alpha} = \frac{3\gamma_{\alpha}\lambda_{\alpha}^3 n_{\text{H}} x_{\text{HI}}}{2H}, \quad (16)$$

³ Note the misprint in Equation (10) of Chuzhoy & Shapiro (2006): inside the integral the argument of exponent should have a z^3 instead of x^3 .

⁴ We find a discrepancy in the Voigt parameter, a , by CM04. The denominator should have 4 instead of 8.

where γ_α is the half width at half maximum of Ly α resonance line given by (H06)

$$\gamma_\alpha = \frac{e^2 \mathcal{F}_\alpha \nu_\alpha^2}{6m_e c^3 \varepsilon_0} = 50 \text{ MHz}, \quad (17)$$

where e is the charge of electron, m_e is its mass, ε_0 is the permittivity of vacuum and $\mathcal{F}_\alpha = 0.4182$ is the oscillator strength of Ly α resonance. Usually the functions J are written in terms of Sobolev parameter γ related to τ_α as $\gamma = \tau_\alpha^{-1}$.

Figure 1 shows the spectra J . The asymmetry in the spectrum can be explained qualitatively as follows. Because of the Doppler effect, when the source and detector are moving towards each other the apparent frequency measured by the detector increases and when moving away it decreases. When a hydrogen atom in the IGM is hit with a radiation, it will selectively absorb photons of frequency ν_α as measured in its rest frame. The resulting spectrum would of course be a Lorentzian in the rest frame. If the Universe was static then this spectrum would still be symmetric when transformed to the lab frame, although it will be more broadened due to the Doppler broadening. However, in an expanding Universe even the sources are also moving and away. Thus, the whole spectrum would come out to be shifted to a higher frequency in order to compensate for this added cosmological redshift.

With the specific intensity function at hand we can now discuss the coupling x_α , colour temperature T_α and then the heating by Ly α photons. The probability that a Ly α photon will bring the H I from the upper hyperfine state to a lower one (indirectly, via WF effect) is approximately 4/27 so that if P_α is the total rate of Ly α photon scattering per hydrogen atom then (H06, Meiksin 2000)

$$P_{10} = \frac{4}{27} P_\alpha. \quad (18)$$

The definition of P_α is

$$P_\alpha = \frac{\pi e^2 \mathcal{F}_\alpha}{m_e \varepsilon_0 c} \int_{-\infty}^{\infty} J(\nu) \phi_\alpha(\nu) d\nu, \quad (19)$$

where $\phi_\alpha(\nu)$ is the normalised Ly α line profile. In the wing approximation it looks like (expressing in terms of dimensionless frequency x)

$$\phi_\alpha(x) \approx \frac{a}{\pi x^2}. \quad (20)$$

Using Equations (18) and (19) in Equation (6) we get

$$x_\alpha = \frac{4\pi e^2 \mathcal{F}_\alpha}{27 A_{21} m_e \varepsilon_0 c} \frac{T_\gamma}{T_\gamma} \int_{-\infty}^{\infty} \frac{J(\nu)}{J_\alpha} \phi_\alpha(\nu) d\nu \quad (21)$$

$$x_\alpha = S \frac{J_\alpha}{J_0}, \quad (22)$$

where S is called the scattering correction given as

$$S = \int_{-\infty}^{\infty} \frac{J(\nu)}{J_\alpha} \phi_\alpha(\nu) d\nu, \quad (23)$$

and

$$J_0 = \frac{27 A_{21} m_e \varepsilon_0 c}{4\pi e^2 \mathcal{F}_\alpha} \frac{T_\gamma}{T_\gamma} \quad (24)$$

$$\approx 5.516 \times 10^{-8} (1+z) \text{ m}^{-2} \text{ s}^{-1} \text{ Hz}^{-1} \text{ sr}^{-1}, \quad (25)$$

where we used $T_\gamma = T_0(1+z)$. An accurate formula for S can be obtained by assuming that line profile is sharply peaked at $\nu = \nu_\alpha$ or equivalently $x = 0$ so that $S \approx J_i(x=0)/J_\alpha$. The

trick to find $J_i(0)$ and hence S is to exploit the continuity of specific intensity of injected photons at $x = 0$.

$$J_i(0) = \frac{2\pi J_\alpha}{a\tau_\alpha} \int_{-\infty}^0 y^2 \exp \left[2\eta y + \frac{2\pi y^3}{3a\tau_\alpha} \right] dy \quad (26)$$

$$S = \frac{2\pi}{a\tau_\alpha} \int_{-\infty}^0 y^2 \exp \left[2\eta y + \frac{2\pi y^3}{3a\tau_\alpha} \right] dy. \quad (27)$$

Different closed form expressions can be found in literature for S (cf. Chuzhoy & Shapiro 2006 and FP06). We derive yet another expression (Appendix A), which is more condensed, given by

$$S = 1 - {}_3F_0(1/3, 2/3, 1; 0; -\xi_1), \quad (28)$$

where

$$\xi_1 = \frac{9\pi}{4a\tau_\alpha\eta^3}, \quad (29)$$

and ${}_3F_0$ is the (3, 0)–hypergeometric function (Chap. 18, Arfken et al. 2013). A typical value of S would be ~ 0.7 at $(z, x_e, T_K) \sim (22, 0, 10 \text{ K})$.

The formal definition of colour temperature is (Rybicki 2006)

$$T_\alpha^{-1} = -\frac{k_B}{h} \frac{d \ln \mathcal{N}(\nu)}{d\nu}, \quad (30)$$

where $\mathcal{N}(\nu) = c^2 J(\nu)/(2\nu^2)$ is the photon occupation number⁵. Clearly, T_α is a frequency dependent quantity. So to calculate an effective colour temperature, it should be averaged over the line profile ϕ_α (Meiksin 2006). However, the difference is really small and the approximation used for S works here as well. The final expression we will use is (Chuzhoy & Shapiro 2006)

$$T_\alpha = T_s \left(\frac{T_K + T_{se}}{T_s + T_{se}} \right), \quad (31)$$

where

$$T_{se} = \left(\frac{\nu_{21}}{\nu_\alpha} \right)^2 \frac{m_H c^2}{9k_B} \approx 0.4 \text{ K}. \quad (32)$$

The smallness of T_{se} is indicative of the fact that for high temperatures the argument of Field (1958) is quite accurate. Thus it is safe to make the statement that the Ly α radiation couples the spin and kinetic temperature. We can eliminate T_α from Equation (4) and write the spin temperature as

$$T_s^{-1} = \frac{T_\gamma^{-1} + x_K T_K^{-1} + x_\alpha (T_K + T_{se})^{-1}}{1 + x_K + x_\alpha T_K (T_K + T_{se})^{-1}}. \quad (33)$$

The spin exchange correction is captured by the term T_{se} . It also modifies the recoil parameter and the Sobolev parameter but here we are neglecting those effects since they are important only at extremely low temperatures, typically $T_K \lesssim 1 \text{ K}$ (FP06).

2.2 Heating by Ly α Photons

We now consider the role of Ly α photons in heating the IGM. We can qualitatively understand it as follows. The continuum

⁵ The photon occupation number should not be confused with the specific number density of photon often denoted by $n(\nu)$ or n_ν . They are related as $n(\nu) = 8\pi\nu^2 \mathcal{N}(\nu)/c^3$.

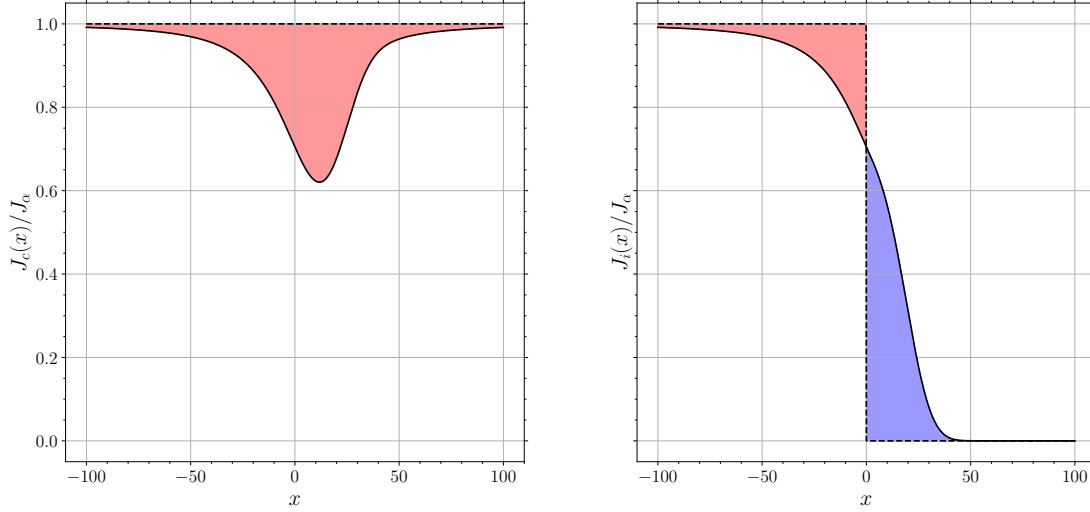


Figure 1. Specific intensity of continuum and injected Ly α photons normalised to the same background intensity. These curves are plotted at $(z, x_e, T_K) \sim (22, 0, 10 \text{ K})$. The left panel shows continuum photons (Equation 10). The right panel shows injected photons (Equation 11). The blue shaded area represents cooling ($I_i^{\text{cool}} \approx -13.07$), while the red one represents heating ($I_i^{\text{heat}} \approx 7.32$). The asymmetry exists because of the extra cosmological redshift due to the expanding Universe. See text for more details. The dashed lines correspond to the case for no scattering of Ly α photons, or the infinite temperature limit.

photons descend from higher frequency and are preferentially scattered off by atoms moving away from them. As a result they continually lose energy and hence cause heating. Stated differently, in the absence of scattering the spectral distortion would redshift away. However, in steady state the photons would lose energy to atoms continuously. In the case of injected photons, some of them are scattered off to the blue side by the atoms moving in the opposite direction which create a cooling effect, while the remaining are scattered off to the red side, which produce a heating effect. The net effect by the continuum and injected photons is quite small compared to X-ray heating because of which it is usually ignored in calculations.

The heat supplied by the continuum photons per unit time per unit proper volume is given by (CM04⁶)

$$q_c = \frac{4\pi}{c} H h \int_{-\infty}^{\infty} \nu (J_\alpha - J_c) d\nu. \quad (34)$$

To simplify calculations, it is assumed that the absorption feature is sharply peaked near Ly α resonance so that ν can be taken outside the integral and set to $\nu = \nu_\alpha$, the frequency of Ly α line. Also, by changing the variable to $x = (\nu - \nu_\alpha) / \Delta\nu_D$ we can write

$$\frac{2q_c}{3nk_B H} = \frac{8\pi}{3} \frac{h\nu_\alpha}{k_{BC}} \frac{J_\alpha \Delta\nu_D}{n(z)} I_c, \quad (35)$$

where

$$I_c = \int_{-\infty}^{\infty} \left[1 - \frac{J_c(x)}{J_\alpha} \right] dx. \quad (36)$$

We have explicitly shown the z dependence of n on the

⁶ There is a typo in Equation (10) of CM04. The factor $\Delta\nu_D$ should not be present. Their equations (17) & (18), however, are correct.

right hand side to remind ourselves that both J_α and n are in proper units. Graphically, I_c is an area between the undisturbed Ly α spectrum (which is a flat line) and a scattered one. See, for e.g., the left panel of Figure 1 plotted at $(z, x_e, T_K) \approx (22, 2.19 \times 10^{-4}, 10 \text{ K})$ in which the red shaded area is $I_c \approx 20.11$. The expression for I_c can be written in a closed form as (FP06)

$$I_c = \eta (2\pi^4 a^2 \tau_\alpha^2)^{1/3} [\text{Ai}^2(-\xi_2) + \text{Bi}^2(-\xi_2)], \quad (37)$$

where

$$\xi_2 = \eta \left(\frac{4a\tau_\alpha}{\pi} \right)^{1/3}, \quad (38)$$

$\text{Ai}(x)$ and $\text{Bi}(x)$ represent the Airy function of first and second kind, respectively (Weisstein 2020).

We can also write an equation similar to Equation (35) for injected photons by changing subscript ‘c’ to ‘i’. However, the I_i is defined as

$$I_i = \int_{-\infty}^0 \left[1 - \frac{J_c(x)}{J_\alpha} \right] dx - \int_0^{\infty} \frac{J_i(x)}{J_\alpha} dx. \quad (39)$$

The first integral in I_i can only be simplified to

$$\int_{-\infty}^0 \left[1 - \frac{J_c(x)}{J_\alpha} \right] dx = \eta \sqrt{\frac{a\tau_\alpha}{2}} \int_0^{\infty} \left[\exp \left(-2\eta y - \frac{\pi y^3}{6a\tau_\alpha} \right) \times \text{erfc} \sqrt{\frac{\pi y^3}{2a\tau_\alpha} \frac{dy}{\sqrt{y}}} \right], \quad (40)$$

where $\text{erfc}(x)$ represents the complementary error function (Chap. 13, Arfken et al. 2013). The second integral is

$$\int_0^{\infty} \frac{J_i(x)}{J_\alpha} dx = \frac{J_i(0)}{J_\alpha} \int_0^{\infty} \exp \left[-2\eta x - \frac{2\pi x^3}{3a\tau_\alpha} \right] dx. \quad (41)$$

We already approximated S by $J_i(0)/J_\alpha$. As for the integral,

we split the exponential into two and do integration by parts to get

$$-\frac{1}{2\eta} \exp \left[-2\eta x - \frac{2\pi x^3}{3a\tau_\alpha} \right] \Big|_0^\infty + \frac{1}{2\eta} \frac{2\pi}{a\tau_\alpha} \int_0^\infty x^2 \exp \left[-2\eta x - \frac{2\pi x^3}{3a\tau_\alpha} \right] dx \quad (42)$$

$$= \frac{1}{2\eta} - \frac{S}{2\eta}, \quad (43)$$

where in the second term we changed the variable to $x = -y$ to get the integral for S as in step (27). So finally we get,

$$I_i = \eta \sqrt{\frac{a\tau_\alpha}{2}} \int_0^\infty \exp \left[-2\eta y - \frac{\pi y^3}{6a\tau_\alpha} \right] \operatorname{erfc} \sqrt{\frac{\pi y^3}{2a\tau_\alpha}} \frac{dy}{\sqrt{y}} - \frac{S(1-S)}{2\eta}. \quad (44)$$

with S being given in Equation (28). Generally, the effect of injected photons is to cool the IGM except at extremely low gas kinetic temperature, typically $T_K \lesssim 1$ K, but such low temperatures are not realised in Λ CDM cosmology. For the example shown in the right panel of Figure 1, $I_i \approx -5.75$.

In the preceding discussion we assumed that the background intensity of continuum and injected photons is the same but this is not true in general. However, we can easily correct for this by specifying the ratio J_α^i/J_α^c , which depends on the surface temperature of the source. We take

$$\frac{J_\alpha^i}{J_\alpha^c} = 0.1, \quad (45)$$

appropriate for Population II (Pop II) type stars (Chuzhoy & Shapiro 2007, hereafter CS07). For comparison, CM04 used $J_\alpha^i/J_\alpha^c = 1$. The final term to be inserted into Equation (8) is

$$\frac{2q_\alpha}{3nk_B H} = \frac{8\pi h\nu_\alpha}{3} \frac{J_\alpha(z)\Delta\nu_D}{k_{BC} n(z)} \left(I_c + \frac{J_\alpha^i}{J_\alpha^c} I_i \right). \quad (46)$$

We ignore the small recoil heating contribution from deuterium atom (CS07).

2.3 The Background Ly α Specific Intensity

To calculate $J_\alpha(z)$ we need the comoving UV emissivity $\epsilon_{UV}(E, z)$. The comoving emissivity is defined as the number of photons emitted per unit comoving volume per unit proper time per unit energy at redshift z and energy E . To model it we assume that it is proportional to the star formation rate density (SFRD) and spectral energy distribution (SED) (Barkana & Loeb 2005). More precisely, Emissivity = (the number of UV photons emitted per unit energy at E per baryon in the stars) \times (number of baryons accumulating in the stars per unit time per unit comoving volume at z), i.e.,

$$\epsilon_{UV}(E, z) = \epsilon_b(E) \frac{\dot{\rho}_*(z)}{m_b}, \quad (47)$$

where $\epsilon_b(E)$ is the SED, defined as the number of photons emitted per baryon per unit energy and m_b is the average baryon mass. For the redshift range of our interest we can accurately write $m_b = 1.22m_H$ (Ali-Haïmoud et al. 2014).

The SED depends on the source or the type of star but it

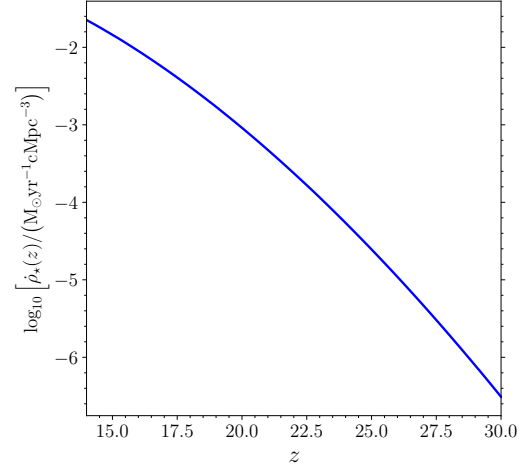


Figure 2. The comoving star formation rate density for a star formation efficiency of $f_* = 0.1$ and halo virial temperatures of $T_{\text{vir}} \geq 10^4$ K.

is generally a broken power law, i.e., $\epsilon_b(E) \propto E^{s-1}$ where the index s can be different between different Lyman lines. We assume the model of Pop II stars which emit $N_{\alpha\beta} = 6520$ photons per baryons between Ly α and Ly β with index $s = 0.14$. Between Ly β and Ly ∞ they emit $N_{\beta\infty} = 3170$ photons per baryons, so that the total is $N_{\alpha\infty} = 9690$ (Barkana & Loeb 2005). To find the proportionality constants and the index for the latter case we used the normalisation and continuity at $E_\beta = 12.09$ eV, which is the energy of the Ly β line. We derive the final expression for ϵ_b in eV^{-1}

$$\epsilon_b(E) = \begin{cases} 2902.91 \hat{E}^{-0.86} & \text{if } E \in [E_\alpha, E_\beta] \\ 1303.34 \hat{E}^{-7.66} & \text{if } E \in (E_\beta, E_\infty], \end{cases} \quad (48)$$

where $\hat{E} = E/E_\infty$, $E_\alpha = 10.2$ eV and $E_\infty = 13.6$ eV are the energies corresponding to Ly α and Ly ∞ transition, respectively.

The comoving SFRD is represented by $\dot{\rho}_*(z)$, and is measured in mass per unit time per unit comoving volume. We assume it is proportional to the rate at which baryons collapse into dark matter haloes. Assuming only the haloes of virial temperatures (T_{vir}) above 10^4 K contribute, their number at a given redshift can be determined by the Press & Schechter (1974) formalism. Thus,

$$\dot{\rho}_*(z) = -(1+z)\bar{\rho}_b^0 f_* H(z) \frac{dF_{\text{coll}}(z)}{dz}, \quad (49)$$

where

$$\bar{\rho}_b^0 = \frac{3H_0^2}{8\pi G} \Omega_b, \quad (50)$$

is the mean cosmic baryon mass density measured today, $f_*(=0.1)$ is the star formation efficiency – defined as the fraction of baryons converted into stars in the haloes – and $F_{\text{coll}}(z)$ is the fraction of baryons that have collapsed into dark matter haloes (Barkana & Loeb 2001, 2005; Furlanetto 2006; Pritchard & Furlanetto 2006). See Figure 2 for a plot of the SFRD as a function of redshift.

It is a good approximation to account for the effect of

higher Lyman series (Lyn) photons only in the total Ly α intensity, since analogous WF effect of Lyn or the direct heating by them is negligible (FP06, however, see Meiksin (2010) for a different point of view). We can now write J_α as

$$J_\alpha(z) = \frac{c}{4\pi} (1+z)^2 \sum_{N=2}^{23} P_N \int_z^{z_{\max}} \frac{\epsilon_{UV}(E'_N, z')}{H(z')} dz', \quad (51)$$

where the N^{th} term in the sum accounts for the finite probability P_N with which a photon in the upper Lyman lines will redshift to Ly α wavelength. The values of P_N are computed in an iterative fashion using the selection rule and the decay rates. The detailed procedure and table of values can be found in H06 or Pritchard & Furlanetto (2006). The redshifted energy of N^{th} Lyman series line is given by

$$E'_N = E_N \frac{1+z'}{1+z}, \quad (52)$$

where E_N is the frequency of the photon released in transition from N^{th} state to ground state:

$$E_N = 13.6 \left(1 - \frac{1}{N^2}\right) \text{ eV}. \quad (53)$$

The maximum redshift from which this photon could have been received is given by

$$1 + z_{\max} = \frac{E_{N+1}}{E_N} (1+z) = \frac{1 - (1+N)^{-2}}{1 - N^{-2}} (1+z). \quad (54)$$

In writing the Equation (51) we implicitly assumed that the Ly α stream freely across the IGM and reach the line centre at the same distance from the source. However, in reality Ly α radiation would suffer multiple scatterings with hydrogen atoms and set up a stable background at different distances from the source. Formally, there should be a distance dependent transmission probability factor to account for this effect (Chuzhoy & Zheng 2007; Semelin et al. 2007; Naoz & Barkana 2008; Reis et al. 2020). We are ignoring these complications here.

3 RESULTS AND ANALYSIS

We now consider the magnitude of Ly α heating expected under our model assumptions. In order to gauge the strength of the Ly α background we parameterize the SED using a scaling parameter f_α (cf. GM19). We introduce this parameter by writing ϵ_b as $f_\alpha \epsilon_b$ so that

$$\epsilon_{UV}(E, z) = f_\alpha \epsilon_b(E) \frac{\dot{\rho}_*(z)}{m_b}, \quad (55)$$

Note how the effect of this change propagates

$$f_\alpha \rightarrow \epsilon_b(E) \rightarrow \epsilon(E, z) \rightarrow J_\alpha \rightarrow x_\alpha, q_\alpha.$$

Thus both the coupling and heating are affected as we change f_α . We will consider six values for it: $f_\alpha = \{0, 10^{-2}, 10^{-1}, 1, 10, 10^2\}$.

Figure 3 shows our result. In the left panel of Figure 3 we show the variation of gas kinetic temperature for different values of f_α . The corresponding plots of differential brightness are shown in the right panel of the same figure. Note how the timing and the depth of the absorption feature changes as f_α is changed. The case $f_\alpha = 0$ corresponds to a Universe where there is no Ly α radiation so that $q_\alpha, x_\alpha = 0$. In such a

scenario the matter temperature just falls as $(1+z)^2$ as expected for pure adiabatic cooling and the 21 cm signal would be practically a null signal (shown in thick red). This is because the collisional coupling x_K in this era is very small and hence the spin temperature is close to CMB temperature. In the right panel of Figure 3 we have also shown the global 21 cm signal reported by the EDGES collaboration (Bowman et al. 2018) in grey dashed line.

Our important finding is that for similar astrophysical assumptions ($f_\alpha = 1$), we find a much reduced Ly α heating than recent literature. As an example, for $f_\alpha = 1$, in the GM19 model Ly α heating becomes significant at $z \sim 22$ while in our case Ly α heating remains subdominant until $z \sim 16$. At $z = 14$, the IGM temperature in our model is an order of magnitude lower ($T_K \sim 6$ K) than that in GM19. This obviously affects the 21 cm signal absorption feature which in our model occurs at $z \sim 16$ and has an amplitude of -220 mK.

GM19 claim that larger values of f_α are ruled out, however, our results say otherwise. If we want the signal to be more negative than from Equation (1) we can say that T_s should be as small as possible. But from Equation (4) the theoretical minimum of T_s can only be the lowest of all quantities being averaged, which here is T_K . For this to happen the weight factor x_α should be as high as possible since $x_K \approx 0$. For e.g., when $f_\alpha = 1$ then at $z = 22$ we get $(x_e, T_K) = (2.19 \times 10^{-4}, 10.14 \text{ K})$ for which $x_\alpha \approx 0.24$ whereas $x_K \approx 3.2 \times 10^{-3}$. Thus, in view of the EDGES signal (Bowman et al. 2018) we can conclude that the optimum strength of Ly α background for Pop II stars would be characterised by

$$1 < f_\alpha < 10, \quad (56)$$

and that too without any excess cooling models such as a phenomenological cooling (Mirocha & Furlanetto 2019) or a physically motivated cooling (such as Barkana 2018b). If we include one of those then we could push f_α to even higher values to get stronger coupling at a negligible cost of extra Ly α heating. We therefore conclude that the EDGES measurement does not rule out significant build-up of a Ly α background at cosmic dawn.

We have not varied the other possibly free parameters in this study such as J_α^i/J_α^c , f_\star and T_{vir} . The latter two are degenerate with f_α . Mirocha & Furlanetto (2019) argue that f_\star should take higher values with which we agree but in disagreement with GM19. The ratio J_α^i/J_α^c , however, is an interesting parameter. In this study we chose its value to be 0.1 but if it increases, then the heating effect by continuum photons would get cancelled by the increased cooling by injected photons (see Equation 46) with no decrement in x_α . For the 21 cm signal this means that the absorption feature becomes deeper, which is more favourable for us, again, keeping in mind the EDGES result.

4 CONCLUSIONS

In this work we saw how the Ly α photons affect the 21 cm signal. Their scattering by the neutral hydrogen atoms in the intergalactic medium couples the spin temperature to the gas kinetic temperature via a process known as Wouthuysen-Field effect, which is dominant in the late Universe ($z \lesssim 30$). As a result of this scattering, the recoil produces a heating

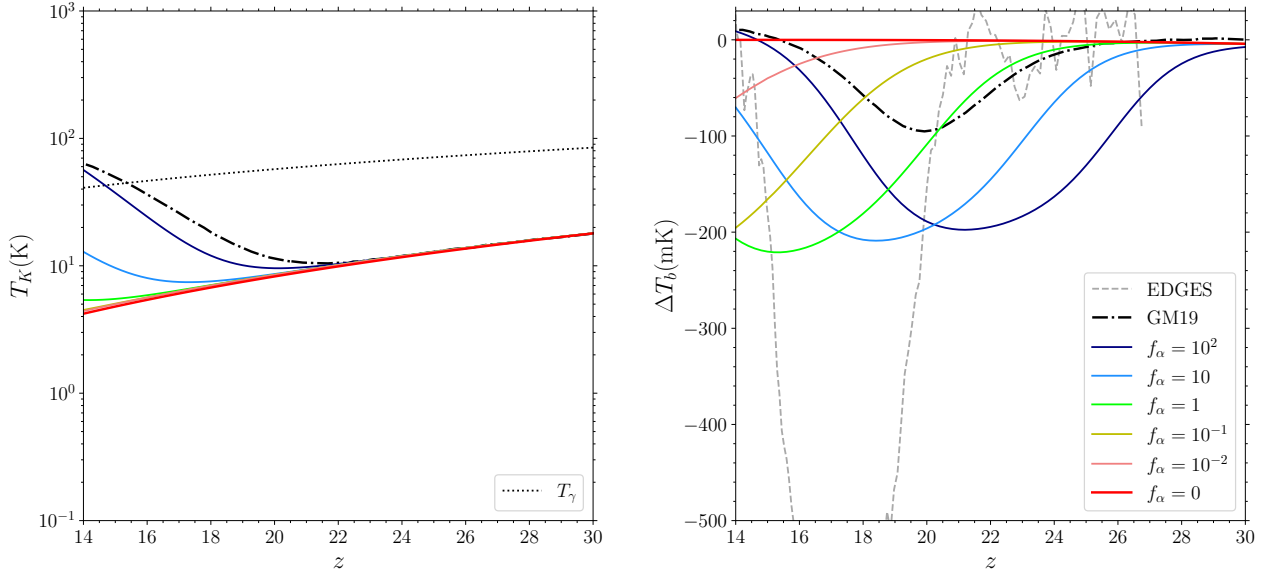


Figure 3. Left panel: gas kinetic temperature T_K evolution. The black dotted line is the CMB temperature $T_\gamma = 2.73(1+z)$. The red solid line ($f_\alpha = 0$) corresponds to the adiabatic cooling in which case $T_K \approx 0.02(1+z)^2$ (Scott & Moss 2009). Right panel: the corresponding differential brightness temperature or the 21 cm signal using Equation (1). The grey dashed line is the EDGES detection of the global 21 cm signal. In both panels the thick black dash dotted line shows the fiducial model from GM19 for comparison.

effect in them. We used the analytical expression for the spectrum of Ly α radiation obtained by wing and Fokker-Planck approximation. Using this expression and a further sharply-peaked nature of line profile it was possible to write the analytical expression for the scattering correction (S) and heating by the continuum photons but not for the heating by injected ones. We derived two new expressions in this work. The first one for S (see Equation 28) and the other being the pure cooling part of injected photons (see Equation 44). We did not involve deuterium anywhere neither did we consider any direct scattering/heating effect of higher Lyman series photons but only accounted for them via radiative cascade in writing the total undisturbed background radiation.

We used the Population II type stars as the source of Ly α radiation. In order to study the effect of their strength on the gas kinetic temperature and hence the differential brightness (the 21 cm signal) we varied the spectral energy distribution by four orders of magnitude but retained its power law. Our key finding in this study is that a strong Ly α background is a necessity in order to produce a strong absorption signal contrary to recent conclusions in the literature. For our fiducial model $f_\alpha = 1$ (the parameter which quantifies the intensity of Ly α background) we find that the IGM remains significantly colder than the CMB down to at least $z = 14$.

The relative strength, sources and their role in 21 cm cosmology of X-ray and ultraviolet radiation is quite uncertain. Each effect bring along its own set of parameters such as f_X , analogous to f_α , which changes the strength of X-ray radiation. We can take this to our advantage and study them over an extensive range to find the model which best fits the EDGES signal as well as satisfies other cosmological constraints (for e.g. Barkana et al. 2018). Some studies which

have taken this approach include Cohen et al. (2017); Greig & Mesinger (2018); Monsalve et al. (2019); Cohen et al. (2020). Some recent papers have provided new insights on old physics such as Meiksin & Madau (2020) who considered an enhanced Ly α radiation from Population III stars which can create a cooling effect if reddened by winds internal to the haloes. Similarly, Mebane et al. (2020) considered effects of X-ray and radio emission from Pop III stars on the 21 cm signal.

We have not attempted to match our signal with that of the EDGES by inserting any exotic cooling or excess radio background models. In future work we will do so and work with a larger redshift range which encompasses not only Ly α heating but also includes the important effects such as photoheating by X-rays (Mesinger et al. 2011, 2013; Christian & Loeb 2013), shock heating (Furlanetto & Loeb 2004), CMB heating (Venumadhav et al. 2018) and models of reionisation (Haardt & Madau 2012).

ACKNOWLEDGEMENTS

It is a pleasure to acknowledge discussions with members of the REACH collaboration. GK gratefully acknowledges support by the Max Planck Society via a partner group grant.

REFERENCES

- Ali-Haïmoud Y., Meerburg P. D., Yuan S., 2014, *Phys. Rev. D*, 89, 083506
- Arfken G. B., Weber H. J., Harris F. E., 2013, *Mathematical Methods for Physicists*, 7 edn. Academic Press, doi:10.1016/C2009-0-30629-7

- Barkana R., 2018a, Galaxy Formation and Evolution. The Encyclopedia of Cosmology Vol. 1, World Scientific, doi:10.1142/9496-vol1
- Barkana R., 2018b, *Nature*, 555, 71
- Barkana R., Loeb A., 2001, *Phys. Rep.*, 349, 125
- Barkana R., Loeb A., 2005, *ApJ*, 626, 1
- Barkana R., Outmezguine N. J., Redigolo D., Volansky T., 2018, *Phys. Rev. D*, 98, 103005
- Berlin A., Hooper D., Krnjaic G., McDermott S. D., 2018, *Phys. Rev. Lett.*, 121, 011102
- Bernardi G., McQuinn M., Greenhill L. J., 2015, *ApJ*, 799, 90
- Bernardi G., et al., 2016, *MNRAS*, 461, 2847
- Bowman J. D., Rogers A. E. E., Monsalve R. A., Mozdzen T. J., Mahesh N., 2018, *Nature*, 555, 67
- Bradley R. F., Tauscher K., Rapetti D., Burns J. O., 2019, *ApJ*, 874, 153
- Chen X., Miralda-Escude J., 2004, *ApJ*, 602, 1
- Christian P., Loeb A., 2013, *JCAP*, 2013, 14
- Chuzhoy L., Shapiro P. R., 2006, *ApJ*, 651, 1
- Chuzhoy L., Shapiro P. R., 2007, *ApJ*, 655, 843
- Chuzhoy L., Zheng Z., 2007, *ApJ*, 670, 912
- Cohen A., Fialkov A., Barkana R., Lotem M., 2017, *MNRAS*, 472, 1915
- Cohen A., Fialkov A., Barkana R., Monsalve R. A., 2020, *MNRAS*, 495, 4845
- Datta K. K., Kundu A., Paul A., Bera A., 2020, Preprint (arXiv:2001.06497)
- Ewall-Wice A., Chang T.-C., Lazio J., Doré O., Seiffert M., Monsalve R. A., 2018, *ApJ*, 868, 63
- Ewall-Wice A., Chang T.-C., Lazio T. J. W., 2019, *MNRAS*, 492, 6086
- Feng C., Holder G., 2018, *ApJ*, 858, L17
- Fialkov A., Barkana R., 2019, *MNRAS*, 486, 1763
- Field G. B., 1958, *Proc. IRE*, 46, 240
- Furlanetto S. R., 2006, *MNRAS*, 371, 867
- Furlanetto S. R., Loeb A., 2004, *ApJ*, 611, 642
- Furlanetto S. R., Pritchard J. R., 2006, *MNRAS*, 372, 1093
- Furlanetto S. R., Peng S., Briggs F. H., 2006, *Phys. Rep.*, 433, 181
- Ghara R., Mellema G., 2019, *MNRAS*, 492, 634
- Grachev S. I., 1989, *Astrophysics*, 30, 211
- Greig B., Mesinger A., 2018, *MNRAS*, 477, 3217
- Gunn J. E., Peterson B. A., 1965, *ApJ*, 142, 1633
- Haardt F., Madau P., 2012, *ApJ*, 746, 125
- Hills R., Kulkarni G., Meerburg P. D., Puchwein E., 2018, *Nature*, 564, E32
- Hirata C. M., 2006, *MNRAS*, 367, 259
- Liszt H., 2001, *A&A*, 371, 698
- Liu H., Outmezguine N. J., Redigolo D., Volansky T., 2019, *Phys. Rev. D*, 100, 123011
- Madau P., Meiksin A., Rees M. J., 1997, *ApJ*, 475, 429
- Mahesh N., Subrahmanyan R., Shankar N. U., Raghunathan A., 2014, Preprint (arXiv:1406.2585)
- Mebane R. H., Mirocha J., Furlanetto S. R., 2020, *MNRAS*, 493, 1217
- Meiksin A., 2000, Detecting the Epoch of First Light in 21-CM Radiation. Perspectives on Radio Astronomy: Science with Large Antenna Arrays, ASTRON
- Meiksin A., 2006, *MNRAS*, 370, 2025
- Meiksin A., 2010, *MNRAS*, 402, 1780
- Meiksin A., Madau P., 2020, Preprint (arXiv:2006.15108)
- Mesinger A., ed. 2019, The Cosmic 21-cm Revolution. 2514-3433, IOP Publishing, doi:10.1088/2514-3433/ab4a73
- Mesinger A., Furlanetto S., Cen R., 2011, *MNRAS*, 411, 955
- Mesinger A., Ferrara A., Spiegel D. S., 2013, *MNRAS*, 431, 621
- Mirocha J., Furlanetto S. R., 2019, *MNRAS*, 483, 1980
- Monsalve R. A., Fialkov A., Bowman J. D., Rogers A. E. E., Mozdzen T. J., Cohen A., Barkana R., Mahesh N., 2019, *ApJ*, 875, 67
- Muñoz J. B., Loeb A., 2018, *Nature*, 557, 684
- Naoz S., Barkana R., 2008, *MNRAS*, 385, L63
- Nhan B. D., Bradley R. F., Burns J. O., 2017, *ApJ*, 836, 90
- Nhan B. D., Bordenave D. D., Bradley R. F., Burns J. O., Tauscher K., Rapetti D., Klima P. J., 2019, *ApJ*, 883, 126
- Patra N., Subrahmanyan R., Raghunathan A., Shankar N. U., 2013, *Exp. Astron.*, 36
- Philip L., et al., 2019, *J. Astron. Instrum.*, 08, 1950004
- Planck Collaboration et al., 2016, *A&A*, 594, A13
- Press W. H., Schechter P., 1974, *ApJ*, 187, 425
- Price D. C., et al., 2018, *MNRAS*, 478, 4193
- Pritchard J. R., Furlanetto S. R., 2006, *MNRAS*, 367, 1057
- Pritchard J. R., Furlanetto S. R., 2007, *MNRAS*, 376, 1680
- Pritchard J. R., Loeb A., 2012, *Rep. Prog. Phys.*, 75, 086901
- Reis I., Barkana R., Fialkov A., 2020, Preprint (arXiv:2008.04914)
- Rybicki G. B., 2006, *ApJ*, 647, 709
- Rybicki G. B., dell'Antonio I. P., 1994, *ApJ*, 427, 603
- Scott D., Moss A., 2009, *MNRAS*, 397, 445
- Seager S., Sasselov D. D., Scott D., 1999, *ApJ*, 523, L1
- Seager S., Sasselov D. D., Scott D., 2000, *ApJS*, 128, 407
- Semelin B., Combes F., Baek S., 2007, *A&A*, 474, 365
- Sims P. H., Pober J. C., 2019, *MNRAS*, 492, 22
- Singh S., Subrahmanyan R., 2019, *ApJ*, 880, 26
- Singh S., et al., 2017, *ApJ*, 845, L12
- Venumadhav T., Dai L., Kaurov A., Zaldarriaga M., 2018, *Phys. Rev. D*, 98, 103513
- Voytek T. C., Natarajan A., García J. M. J., Peterson J. B., López-Cruz O., 2014, *ApJ*, 782, L9
- Weisstein E. W., 2020, Airy Functions, <https://mathworld.wolfram.com/AiryFunctions.html>
- Woodgate G. K., 1983, Elementary Atomic Structure, 2 edn. Oxford University Press
- Wouthuysen S. A., 1952, *AJ*, 57, 31
- de Lera Acedo E., 2019, in 2019 International Conference on Electromagnetics in Advanced Applications (ICEAA). IEEE, pp 0626–0629, doi:10.1109/ICEAA.2019.8879199

APPENDIX A: A DERIVATION FOR THE SCATTERING CORRECTION, S

Here we derive the Equation (28). Starting from Equation (27) we have

$$S = \frac{2\pi}{a\tau_\alpha} \int_{-\infty}^0 y^2 \exp \left[2\eta y + \frac{2\pi y^3}{3a\tau_\alpha} \right] dy. \quad (\text{A1})$$

Make a change of variable: $u = -2\eta y$ and set

$$\xi_1 = \frac{9\pi}{4a\tau_\alpha\eta^3}, \quad (\text{A2})$$

to get

$$S = \int_0^\infty \left[\frac{\xi_1 u^2}{9} e^{-\xi_1(u/3)^3} \right] e^{-u} du. \quad (\text{A3})$$

Integration by parts gives

$$S = 1 - \int_0^\infty e^{-\xi_1(u/3)^3} e^{-u} du. \quad (\text{A4})$$

Make a Taylor's series expansion of the first exponential to get

$$S = 1 - \sum_{n=0}^\infty \frac{1}{3^{3n}} \left[\int_0^\infty u^{3n} e^{-u} du \right] \frac{(-\xi_1)^n}{n!}, \quad (\text{A5})$$

where ‘!’ represents the regular factorial. The integral is the just the gamma function (Chap. 13, Arfken et al. 2013), hence

$$S = 1 - \sum_{n=0}^{\infty} \frac{(3n)!}{3^{3n}} \frac{(-\xi_1)^n}{n!}. \quad (\text{A6})$$

In terms of the Pochhammer symbol or the rising factorial (Chap. 18, [Arfken et al. 2013](#)) the above expression can be rewritten as

$$S = 1 - \sum_{n=0}^{\infty} (1/3)_n (2/3)_n (1)_n \frac{(-\xi_1)^n}{n!}. \quad (\text{A7})$$

By the definition of generalised hypergeometric function

$$S = 1 - {}_3F_0(1/3, 2/3, 1; 0; -\xi_1). \quad (\text{A8})$$

This paper has been typeset from a $\text{\TeX}/\text{\LaTeX}$ file prepared by the author.